Geophysical Research Letters

AN AGU JOURNAL

Volume 42 • Issue 3 • 16 February 2015 • Pages 673–966

AGU PUBLICATIONS

WILEY

AGU PUBLICATIONS

Geophysical Research Letters

RESEARCH LETTER
10.1002/2014GL062280

Key Points:
- First analytical solution for equatorial waves in cyclostrophic regimes
- Explanation for Y feature's morphology, darkness, and time evolution
- Analytical model applicable to exoplanets with atmospheric superrotation

Supporting Information:
- Text S1
- Movie S1
- Figure S1

Correspondence to:
J. Peralta,
peralta@iaa.es

Citation:
Peralta, J., A. Sánchez-Lavega, M. A. López-Valverde, D. Luz, and P. Machado (2015), Venus's major cloud feature as an equatorially trapped wave distorted by the wind, *Geophys. Res. Lett.*, *42*, doi:10.1002/2014GL062280.

Received 21 OCT 2014
Accepted 7 JAN 2015
Accepted article online 11 JAN 2015

Venus's major cloud feature as an equatorially trapped wave distorted by the wind

J. Peralta[1], A. Sánchez-Lavega[2,3], M. A. López-Valverde[1,3], D. Luz[4], and P. Machado[4]

[1]Instituto de Astrofísica de Andalucía (IAA-CSIC), Granada, Spain, [2]Departmento de Física Aplicada I, ETSI (UPV/EHU), Bilbao, Spain, [3]Unidad Asociada GCP UPV/EHU-IAA (CSIC), Bilbao, Spain, [4]Centro de Astronomia e Astrofísica da Universidade de Lisboa, Observatório Astronómico de Lisboa, Lisbon, Portugal

Abstract The superrotation of the atmospheres of slowly rotating bodies is a long-standing problem yet unsolved in atmospheric dynamics. On Venus, the most extreme case known of superrotation, this is accompanied and influenced by a recurrent planetary-scale cloud structure, known as the Y feature. So far, no model has simultaneously reproduced its shape, temporal evolution, related wind field, nor the relation between its dynamics and the unknown UV-absorbing aerosol that produces its dark morphology. In this paper we present an analytical model for a Kelvin-like wave that offers an explanation of these peculiarities. Under Venus cyclostrophic conditions, this wave is equatorially and vertically trapped where zonal winds peak and extends 7 km in altitude, and its vertical wind perturbations are shown to produce upwelling of the UV absorber. The Y-feature morphology and its 30 day evolution are reproduced as distortions of the wave structure by the Venus winds.

1. Introduction

Venus's large-scale dark Y pattern (the Y-tilted 90°, also described as a "Psi") was discovered in the 1960s [*Boyer and Camichel*, 1961], and it has been repeatedly identified in ultraviolet images from many space missions [*Belton et al.*, 1976; *Rossow et al.*, 1980; *Peralta et al.*, 2007a; *Titov et al.*, 2012]. The Y pattern is a recurrent pattern whose lifetime seems to alternate between cycles of creation and destruction [*Rossow et al.*, 1980]. It shows two arms symmetric relative to the equator, extends up to a latitude of 45° (Figure 1a), and it has a quasi-uniform rotation with a period of about four terrestrial days, differing between 0.7 and 0.1 days from the period of the zonal wind at the equator [*del Genio and Rossow*, 1990]. A recent characterization of the wind field associated with the Y feature [*Kouyama et al.*, 2012] showed a good correspondence with the cloud brightness distribution [*Peralta et al.*, 2007a], with westward acceleration occurring in the dark regions (Figure 1b). Previous analytical studies of equatorial waves on Venus relied on the geostrophic formulation by means of a frame of coordinates fixed to the superrotating winds for which solid-body rotation is assumed [*Smith et al.*, 1992; *Covey and Schubert*, 1981; *Imamura*, 2006]. This is not realistic since the zonal wind profile is far from such a rigid rotation [*Rossow et al.*, 1990; *Peralta et al.*, 2007b; *Smith et al.*, 1993]. Moreover, the properties of the equatorial waves in a cyclostrophic regime like the Venusian have never been studied analytically but with complex numerical models involving a difficult interpretation of the phenomenon, and in no case make a successful comparison with the time evolution of the Y feature reported with Pioneer Venus observations [*Smith et al.*, 1992, 1993; *Yamamoto and Tanaka*, 1997, 1998; *Imamura*, 2006; *Lee et al.*, 2010; *Kouyama et al.*, 2015]. Most of the previous works interpret the Y feature as the combination of two modes: a Rossby mode at midlatitudes and a Kelvin mode at the equatorial region [*del Genio and Rossow*, 1990; *Imamura*, 2006; *Kouyama et al.*, 2015], although classical Rossby and Kelvin waves are not possible in cyclostrophic regimes [*Peralta et al.*, 2014b], and periodograms from zonal winds obtained with Venus Express observations do not show evidence of two simultaneous modes at equator and midlatitudes but a single equatorial mode extending to midlatitudes [see *Kouyama et al.*, 2013, Figure 9] and with periods varying between 4 and 5 days [see *Khatuntsev et al.*, 2013, Table 2]. For this reason, we investigate the Kelvin-like wave that could arise as a solution in Venus's particular conditions.

2. An Equatorial Wave for Cyclostrophic Regimes

Our analytical model starts from the primitive equations for a cyclostrophic regime [*Peralta et al.*, 2014a, 2014b] (see Appendix A), neglecting equatorward of midlatitudes the meridional shear of the zonal wind,

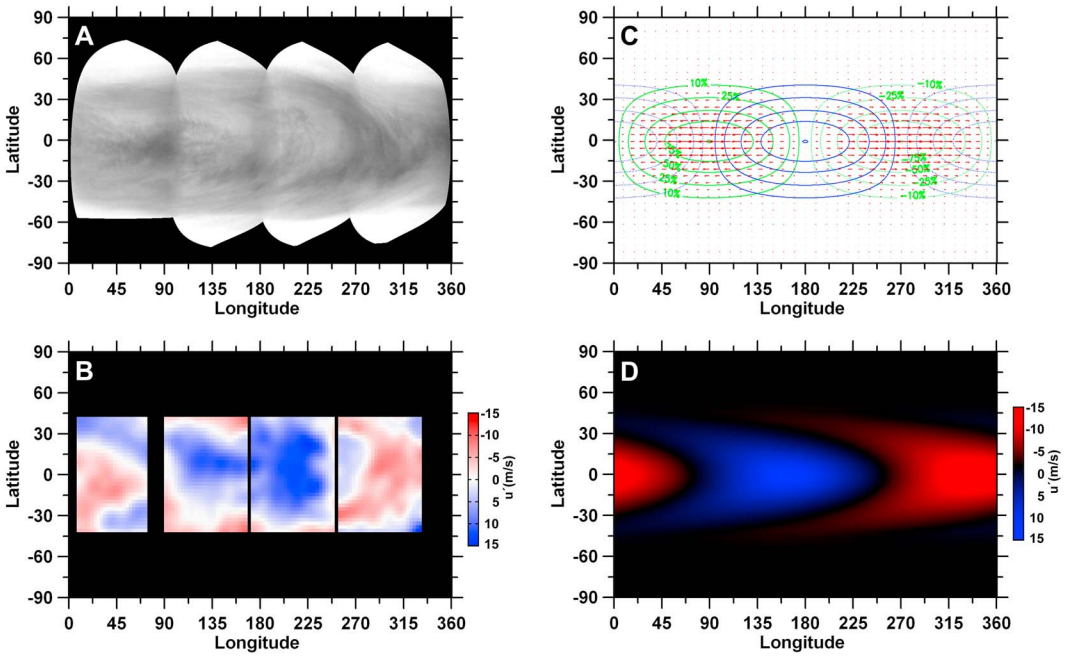

Figure 1. Observations and model of Venus Y pattern. (a) Composite of Venus cloud tops during Galileo flyby [*Peralta et al.*, 2007a]. (b) Zonal wind perturbations during Galileo flyby [*Kouyama et al.*, 2012]. (c) Horizontal structure of our wave according to equations (4)–(6). Zonal wind disturbances (u') are displayed with red arrows. Blue lines display perturbations on pressure (P') and in-phase component of vertical velocity (w'). Green lines show the 90°-shifted component of w'. Lines are percentages of the maximum amplitude, and continuous/dotted lines denote positive/negative disturbances, respectively. (d) Zonal wind disturbances predicted by our wave model after 6 days of propagation within a realistic zonal mean flow.

and incorporating the vertical shear of the zonal wind [*Schubert*, 1983; *Gierasch et al.*, 1997; *Peralta et al.*, 2007b]. While on the Earth, what traps atmospheric waves along the equator is the meridional variation of the Coriolis parameter $f \approx \beta \cdot y$ (with $f = 2\Omega \cdot \sin\phi$, $\beta = \mathrm{d}f/\mathrm{d}y$, with Ω being Earth's angular rotation velocity and y the meridional coordinate) [*Sánchez-Lavega*, 2011], we find that on Venus this role is played by the centrifugal force through a *centrifugal frequency* [*Peralta et al.*, 2014a, 2014b] $\Psi = (u_0 \cdot \tan\phi)/a$ (where ϕ is the latitude, u_0 is Venus background zonal wind, and a is the planetary radius of Venus). Equivalently, Ψ is found to vary linearly between the equator and midlatitudes with ($\Psi \approx \beta_* \cdot y$ with $\beta_* = \partial\Psi/\partial y$) [*Peralta et al.*, 2014b]. Under these conditions, the wave dispersion relation and the e-folding decays for our Kelvin-like wave amplitude are (see Appendix A for demonstration)

$$\bar{c}_x = \frac{-1}{\sqrt{k^2+m^2}} \cdot \sqrt{N^2 - \frac{1}{4}\left(\frac{\mathrm{d}u_0}{\mathrm{d}z}\right)^2} \tag{1}$$

$$\theta^H_{e-\mathrm{fold}} = \left(\frac{\Gamma^2}{2} + \frac{|\beta_*|}{|\bar{c}_x|}\right)^{-1/2} \tag{2}$$

$$\theta^V_{e-\mathrm{fold}} = \frac{2\,|\beta_*|}{\Gamma^2} \cdot \frac{|\mathrm{d}u_0/\mathrm{d}z|}{N^2} \tag{3}$$

where $\theta^H_{e-\mathrm{fold}}$ and $\theta^V_{e-\mathrm{fold}}$ are the horizontal and vertical e-folding decays, $\bar{c}_x < 0$ is the horizontal phase velocity, k and m are the horizontal and vertical wave numbers, N is the Brunt-Väisällä frequency, $\mathrm{d}u_0/\mathrm{d}z$ is the vertical shear of the zonal wind, and $\Gamma^2 > 0$ (with units m^{-2}) is a constant that appears as a consequence of the vertical wind shear, $\mathrm{d}u_0/\mathrm{d}z \neq 0$.

The e-folding decays are expressed relative to the equator and the altitude $z_0 \sim 67$ km where the zonal wind peaks (Figure 2b). According to our reference atmosphere (see Figure 2 and *Peralta et al.* [2014a]), for $z < z_0$ we have that $N^2 \approx 3.6 \cdot 10^{-4}\ \mathrm{s}^{-2}$, $\mathrm{d}u_0/\mathrm{d}z \approx -6.5 \cdot 10^{-3}\ \mathrm{s}^{-1}$ and $\beta_* \approx -2.5 \cdot 10^{-12}\ \mathrm{s}^{-1}\ \mathrm{m}^{-1}$; while for $z > z_0$

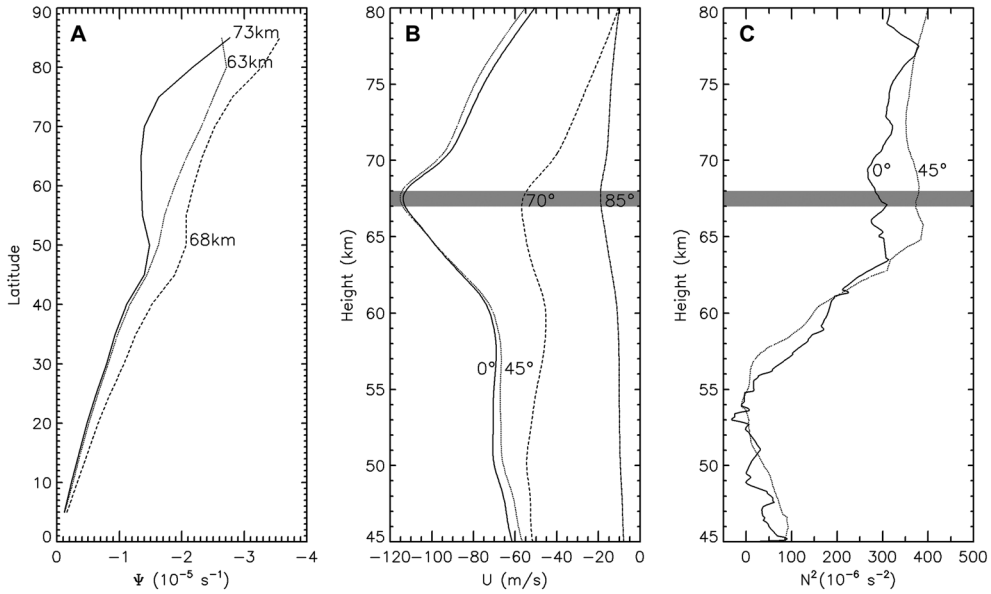

Figure 2. Meridional profile for the centrifugal frequency Ψ at three height levels of (a) the Venus atmosphere and (b) vertical profiles for the background zonal wind and (c) Brunt-Väisällä frequency at several latitudes. The grey area corresponds to the reference altitude z_0 where $du_0/dz = 0$ and the zonal wind peak. Observe that the centrifugal frequency behaves as linear between the equator and midlatitudes. The zonal wind data were taken from our Venus reference atmosphere combining and interpolating horizontal profiles from cloud tracking with vertical profiles obtained with in situ measurements by Pioneer Venus probes [*Peralta et al.*, 2014a].

we obtain $du_0/dz \approx 3.5 \cdot 10^{-3}$ s^{-1}, $\beta_* \approx -2.6 \cdot 10^{-12}$ s^{-1} m^{-1}, and nearly the same value for N^2. Equation (2) predicts that at the altitude level $z = 65$ km the absolute intrinsic phase velocity must fulfill the condition $|\bar{c}_x| > |\beta_*| \cdot (\theta^H_{e-\text{fold}})^2$ and indicates that the meridional width is quite sensitive to the phase velocity. And using the horizontal *e*-folding 2882 ± 427 km obtained during Galileo flyby of Venus [*Kouyama et al.*, 2012] (Figures 1a and 1b and Table 1), we obtain $|\bar{c}_x| > 21.1$ m s^{-1}, which compares well with the phase velocity 23 ± 6 m s^{-1} of the Y feature during the Galileo flyby [*Kouyama et al.*, 2012].

If we take $|\bar{c}_x| = 23$ m s^{-1} [*Kouyama et al.*, 2012], equation (2) gives $\Gamma^2 \approx 1.99 \cdot 10^{-14}$. Then, equation (3) gives $\theta^V_{e-\text{fold}} \approx 2.5$ km and $\theta^V_{e-\text{fold}} \approx 4.5$ km above and below the altitude z_0, respectively, implying for the wave a net vertical envelope of ~7 km. This vertical extent can be compared with the vertical wavelength given by equation (1) for the Y feature having zonal wave number 1 [*Schubert*, 1983; *Gierasch et al.*, 1997;

Table 1. Venus Y-Feature Wave Properties

Wave Description	Measurements[a]	Model
Period (ground based) ($\tau = 2\pi/\omega$)	3.94–4.00 days	3.7 days
Zonal wave number ($s = k \cdot a \cos\phi$)	1	1
Vertical wavelength ($\lambda_z = 2\pi/m$)	—	7.6 km
Zonal velocity (65 km)	95 ± 2 m s^{-1}	100 m s^{-1}
Intrinsic phase velocity (relative to zonal flow)	16 ± 5 m s^{-1}	23 m s^{-1}
$\hat{u}$	9 ± 1 m s^{-1}	10 m s^{-1}
$\hat{P}$	—	32.9 Pa
$\hat{w}$	—	$1.6 \cdot 10^{-3}$ m s^{-1}
Horizontal *e*-folding	2882 ± 427 km	2880 km
Vertical scale	—	7 km

[a]Measurements derived from cloud albedo [*del Genio and Rossow*, 1990] and winds [*Kouyama et al.*, 2012].

Peralta et al., 2007a] ($m \gg k$). At 65 km height we have $\lambda_z \approx 7.6$ km, which is compatible with our predicted vertical length. This value also constrains the nature of the UV absorber since its weighting function should be narrower than $\lambda_z/2$ for the Y feature to be visible [*del Genio and Rossow*, 1990].

For constant du_0/dz and N^2 (see Figures 2b and 2c), the wave's amplitude on the pressure, and zonal and vertical velocity is given by (see Appendix A for demonstration)

$$\hat{P} = \hat{P}_0 \cdot \exp\left[-\left(\frac{\Gamma^2}{2} + \frac{|\beta_*|}{|\bar{c}_x|}\right) \cdot y^2\right] \cdot \exp\left[-\frac{\Gamma^2 N^2}{2|\beta_*|} \cdot \frac{(z - z_0)}{du_0/dz}\right] \cdot e^{i \cdot m \cdot z} \tag{4}$$

$$\hat{u} = \left(\frac{\Gamma^2}{2|\beta_*|} + \frac{1}{|\bar{c}_x|}\right) \cdot e^{i \cdot \pi} \cdot \frac{\hat{P}}{\rho_0} \tag{5}$$

$$\hat{w} = \left(\frac{|\bar{\omega}|}{N^2} m\right) \cdot \frac{\hat{P}}{\rho_0} + \left(\frac{\Gamma^2}{2|\beta_*|} \cdot \frac{|\bar{\omega}|}{du_0/dz}\right) \cdot e^{i\frac{\pi}{2}} \cdot \frac{\hat{P}}{\rho_0} \tag{6}$$

where $\hat{P}_0 = \hat{P}(0, z_0)$ and ρ_0 is the density of the basic state. Equation (4) indicates that the altitude z_0 represents an upper limit for this equatorial wave propagation: $du_0/dz > 0$ for $z > z_0$ means that the wave amplitude exponentially decreases with altitude, while $du_0/dz < 0$ for $z < z_0$ implies that the wave amplitude decreases exponentially but with depth. Accordingly, the wave stays vertically trapped in the layer of maximum background wind speed, which is also where more than a half of the solar energy is absorbed [*Gierasch et al.*, 1997]. On the other hand, from (5) wave disturbances u' and P' are phase shifted 180° implying that the phase of westward acceleration ($u' < 0$) corresponds to increasing pressure ($P' > 0$) and decreasing geopotential height. Our estimates for the wave amplitude (Table 1) can be checked to have values less than 1% of the nominal value in the case of the pressure and vertical velocity, while in the case of the zonal wind perturbations they reach up to 10%, as predicted by *Seiff et al.* [1985], barely affecting the cyclostrophic balance.

3. Differences With the Geostrophic Kelvin Wave

Even though the equatorial wave hereby deduced keeps similarities with the terrestrial Kelvin waves (it propagates along the west-east direction and is equatorially trapped, its wave amplitude is maximum at the equator and decreases away from it), it also presents distinct properties that arise from the absence of the Coriolis factor on Venus and clearly set its different nature. Equation (1) indicates that the wave propagates in the same sense as the mean zonal flow, thus implying that it moves to the west while Kelvin waves on the Earth propagate eastward. The polarization relation (4) contains information about both the meridional and vertical modulations of the wave amplitude. In the presence of vertical shear ($\Gamma \neq 0$) with a local maximum (Figure 2b), our wave is also vertically trapped about a certain altitude. Moreover, when the horizontal *e*-folding decay for the Kelvin waves [*Sánchez-Lavega*, 2011] is confronted with equation (2), we notice that they have different expressions. This is reasonable as the nature of the agent responsible of trapping the waves about the equator is completely different on both planets, i.e., the change of sign for the Coriolis factor f on the Earth, while in the Venus case that role is played by the centrifugal frequency, Ψ. Moreover, the dependence between the phase velocity and meridional width clearly differs from that for the Kelvin waves since on Venus we have different values of β_* and a wider range of validity for the β-plane approximation (see Figure 2a).

4. The Dark Appearance of the Y Feature

It is still unclear whether the cause for the dark contrasts observed in ultraviolet is due to differences in cloud top altitude, temperature contrasts, or compositional variations, with the later being probably related with small aerosol concentrations of reflectors [*Yamamoto and Tanaka*, 1998] or enhanced concentrations of an UV absorber [*Rossow et al.*, 1980; *del Genio and Rossow*, 1990; *Titov et al.*, 2008]. Based on recent evidence from Venus Express observations [*Titov et al.*, 2008], here we assume that contrasts are caused by upwelling of an absorber from a depth which is yet to be determined accurately [*Molaverdikhani et al.*, 2012] and that convective mixing cannot be the only agent for this upwelling since a permanent solar-locked dark feature attached to the subsolar point would be observed then [*Rossow et al.*, 1980]. Figures 1c and 1d show that our

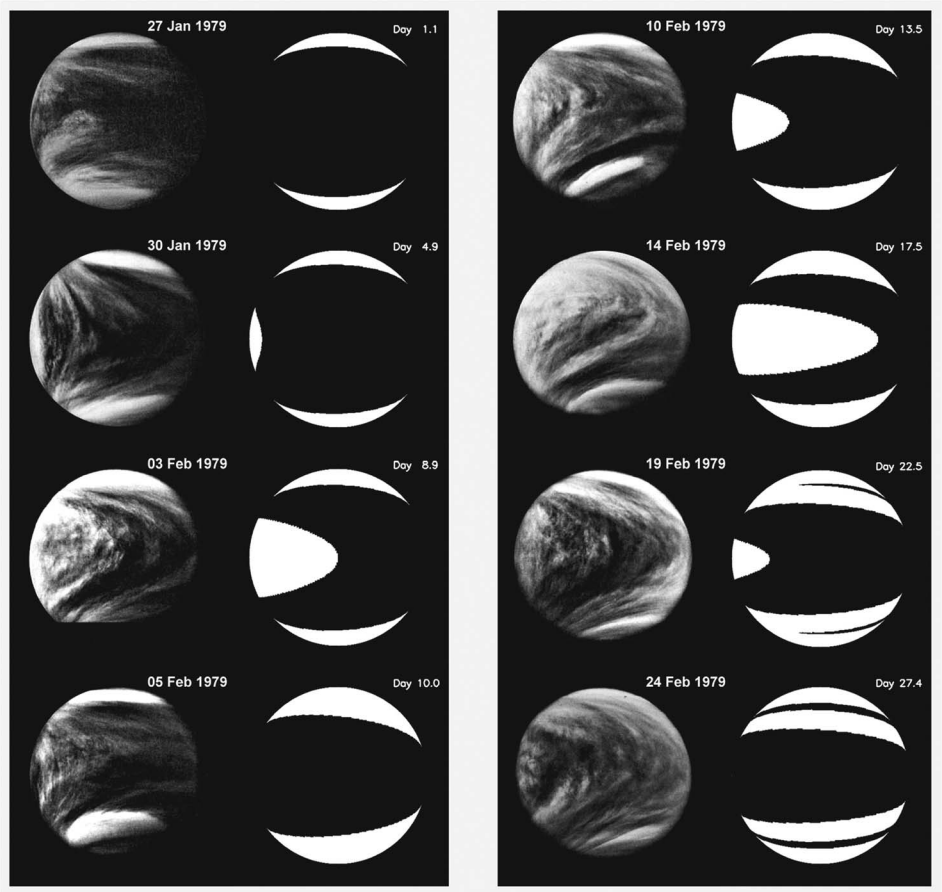

Figure 3. Evolution of Venus Y pattern and the wave model. The Y feature during the Pioneer Venus mission [*Rossow et al.*, 1980] is compared with the evolution of the wave's horizontal structure shown in Figure 1c when propagating within Venus' winds. To fit the geometry of observations, spacecraft projections of the wave model were made with line of sight intersecting the equator. The wave phase with high concentrations of the absorber due to the upwelling is displayed with a single tone of black, while the phase associated to the downwelling and where wave's amplitude is less than 1% of maximum are displayed in white to enhance contrast and improve comparison.

model's P' and u' match the observed cloud albedo field and the horizontal wind field (Figures 1a and 1b). This evident correlation supports previous works' interpretation of dark features as the result of upwelling of the ultraviolet absorber by vertical wind perturbations over a half cycle of the wave, while bright features are the result of downwelling of absorber-depleted air over the other half cycle [*Belton et al.*, 1976; *del Genio and Rossow*, 1990; *Kouyama et al.*, 2012]. Nevertheless, maximum pressure and vertical velocity amplitudes (equations (4) and (6)) are $\hat{P}/P_0 \approx 10^{-3}$ and $\hat{w} \approx 1.6 \cdot 10^{-3}$ m s^{-1} (Table 1), so vertical displacements are ~280 m over half a cycle of the equatorial wave (~2days), which is a short distance (<< vertical scale height H) to justify the upwelling causing the high concentrations of ultraviolet absorber. Alternatively, we propose that this upwelling can be provided by the 90°-shifted component of w'. This component is inversely proportional to the vertical shear of the wind (equation (6)), thus allowing $\hat{w}$ to shoot up close to the altitude where the zonal wind peaks and $du_0/dz \to 0$. The lag between the dark region and the phase for maximum upwelling seen in the observations can be explained as a result of the strength of atmospheric molecular diffusion [*del Genio and Rossow*, 1990], not included in this model.

5. Shape and Evolution of the Y Feature

Previous attempts to explain the shape of the Y feature required the resonant interaction between two planetary waves [*Belton et al.*, 1976; *del Genio and Rossow*, 1990; *Yamamoto and Tanaka*, 1997] or a single Kelvin wave with transient convective patterns that explain its morphology only partially [*Smith et al.*, 1992, 1993]. The first hypothesis is supported by the presence of two periods of 4 and 5 days during Pioneer Venus

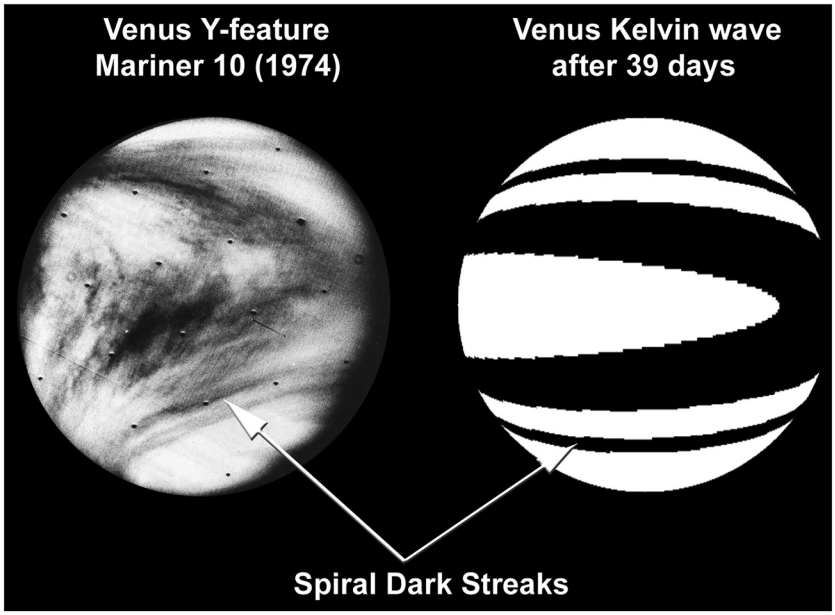

Figure 4. Comparison between (left) the dark circular streaks that appear in the UV images taken during the Mariner 10 flyby of Venus (also, see *Belton et al.* [1976, Figure 6]) and (right) the lag of the wave phase apparent in our simulations after 22 terrestrial days.

observations, although these modes were shown to rule over different latitude ranges which overlap in a narrow region [see *del Genio and Rossow*, 1990, Figure 1]. All theories failed to explain the evolution of the Y along one or several of its life cycles as documented by *Rossow et al.* [1980]. Alternatively, we explain the temporal behavior of the Y feature as the result of the distortion that the equatorial wave (equations (4)–(6)) undergoes when propagating within a realistic zonal flow for Venus [*Peralta et al.*, 2014a]. Since this flow is far from solid-body rotation [*Peralta et al.*, 2007b], the wave's period is shorter at higher latitudes. As a consequence, the coherence of the wave suffers a progressive deformation as it circles the planet (see Movie S1 in the supporting information), consistently with the phase tilt previously reported by *Covey and Schubert* [1982] and *Imamura* [2006]. Figure 3 exhibits the temporal evolution of the wave predicted with our model compared with that of the observed Y feature [*Rossow et al.*, 1980]. The simulation, carried out with time steps of 0.1 terrestrial days and spanning 30 days, covers the 20 day characteristic time based on the energy loss per period for a wave excited by a radiative-dynamic cloud feedback [*Smith et al.*, 1992] and not included in the model. For the background zonal wind between the equator and midlatitudes, we used the mean value -86 m s^{-1} during the data set of Pioneer Venus images [see *Rossow et al.*, 1980, Figure 16a]. An intrinsic phase velocity of 14 m s^{-1} was found to provide an optimum fit to Pioneer Venus observations, also in accordance with the estimation 16 ± 5 m s^{-1} from the cloud brightness [*del Genio and Rossow*, 1990], and implied a horizontal *e*-folding decay of about 2348 km. Except for the slightly different tilt at midlatitudes apparent in Pioneer Venus images, Figure 3 displays quite a good agreement between the cloud morphology and the brightness contrast expected as the equatorial wave becomes distorted. The so-called spiral dark streaks that can be seen at higher latitudes at mature states of the Y feature [see *Belton et al.*, 1976, Figure 6] appear in our simulations at day 22 and are consistent with the increasing lag with latitude of the wave phase (see Figure 4).

6. Conclusions

Despite the many works facing the physical interpretation of the Venus Y feature, none has inferred an analytical model based in the prevailing cyclostrophic conditions. In this paper, we provide a self-consistent model for the equatorial mode of the Y-feature morphology, its 30 day evolution and the appearance of subpolar dark streaks [*Belton et al.*, 1976; *Rossow et al.*, 1980], which are a result of the phase distortion of an equatorially trapped wave as it propagates within the Venus winds. Our wave model is a solution of primitive equations from a scale analysis with Venus Express data [*Peralta et al.*, 2014a] which properly describe the Venus cyclostrophic regime. Along with other waves' solutions previously obtained [*Peralta*

et al., 2014b], our wave model could potentially be extended to other slowly rotating bodies like Titan [*Flasar et al.*, 2010] and the increasing number of extrasolar planets suspected to have, globally or locally, cyclostrophic conditions. Future improvements for this model must include Venus's meridional flow (which may improve the tilt of the dark streaks at midlatitudes), midlatitude interactions with a 5 day mode at midlatitudes in terms of centrifugal waves [*Peralta et al.*, 2014b], as well as exploring the sources of excitation for these equatorial waves.

Acknowledgments

J. Peralta acknowledges the Spanish MICINN for funding support through the CONSOLIDER program "ASTROMOL" CSD2009-00038 and also funding through project AYA2011-23552. A.S.-L. was supported by the Spanish MICIIN project AYA2012-36666 with FEDER support, Grupos Gobierno Vasco IT765-13 and UPV/EHU UFI11/55. P.M. acknowledges the support from Observatoire de Paris-LESIA and the Portuguese Foundation for Science and Technology (FCT, PhD grant reference: SFRH/BD/66473/2009). D.L. and P.M. acknowledge FCT funding through project grants POCI/CTE-AST/110702/2009, PEst-OE/FIS/UI2751/2014, and EC project EuroVenus. Anonymous reviewers are thanked for their fruitful corrections which allowed to greatly improve this paper.

The Editor thanks two anonymous reviewers for their assistance in evaluating this paper.

References

Belton, M. J. S., G. R. Smith, G. Schubert, and A. D. del Genio (1976), Cloud patterns, waves and convection in the Venus atmosphere, *J. Atmos. Sci.*, *33*, 1394–1417.

Boyer, C., and H. Camichel (1961), Observations photographiques de la planète Vénus, *Ann. Astrophys.*, *24*, 531.

Covey, C., and G. Schubert (1982), Planetary-scale waves in the Venus atmosphere, *J. Atmos. Sci.*, *39*, 2397–2413, doi:10.1175/1520-0469(1982)039<2397:PSWITV>2.0.CO;2.

Covey, C. C., and G. Schubert (1981), 4-day waves in the Venus atmosphere, *Icarus*, *47*, 130–138, doi:10.1016/0019-1035(81)90097-X.

del Genio, A. D., and W. B. Rossow (1990), Planetary-scale waves and the cyclic nature of cloud top dynamics on Venus, *J. Atmos. Sci.*, *47*, 293–318.

Flasar, F. M., K. H. Baines, M. K. Bird, T. Tokano, and R. A. West (2010), Atmospheric dynamics and meteorology, in *Titan from Cassini-Huygens*, edited by R. H. Brown, J.-P. Lebreton, and J. HunterWaite, p. 323, Springer, London, doi:10.1007/978-1-4020-9215-2_13.

Gierasch, P. J., et al. (1997), The general circulation of the Venus atmosphere: An Assessment, in *Venus*, edited by S. W. Bougher, D. Hunten, and R. Philips, pp. 459–500, Univ. of Ariz., Tucson.

Imamura, T. (2006), Meridional propagation of planetary-scale waves in vertical shear: Implication for the Venus atmosphere, *J. Atmos. Sci.*, *63*, 1623–1636, doi:10.1175/JAS3684.1.

Khatuntsev, I. V., M. V. Patsaeva, D. V. Titov, N. I. Ignatiev, A. V. Turin, S. S. Limaye, W. J. Markiewicz, M. Almeida, T. Roatsch, and R. Moissl (2013), Cloud level winds from the Venus express monitoring camera imaging, *Icarus*, *226*, 140–158, doi:10.1016/j.icarus.2013.05.018.

Kouyama, T., T. Imamura, M. Nakamura, T. Satoh, and Y. Futaana (2012), Horizontal structure of planetary-scale waves at the cloud top of Venus deduced from Galileo SSI images with an improved cloud-tracking technique, *Planet. Space Sci.*, *60*, 207–216, doi:10.1016/j.pss.2011.08.008.

Kouyama, T., T. Imamura, M. Nakamura, T. Satoh, and Y. Futaana (2013), Long-term variation in the cloud-tracked zonal velocities at the cloud top of Venus deduced from Venus express VMC images, *J. Geophys. Res. Planets*, *118*, 37–46, doi:10.1029/2011JE004013.

Kouyama, T., T. Imamura, M. Nakamura, T. Satoh, and Y. Futaana (2015), Vertical propagation of planetary-scale waves in variable background winds in the upper cloud region of Venus, *Icarus*, *248*, 560–568, doi:10.1016/j.icarus.2014.07.011.

Lee, C., S. R. Lewis, and P. L. Read (2010), A bulk cloud parameterization in a Venus general circulation model, *Icarus*, *206*, 662–668, doi:10.1016/j.icarus.2009.09.017.

Molaverdikhani, K., K. McGouldrick, and L. W. Esposito (2012), The abundance and vertical distribution of the unknown ultraviolet absorber in the Venusian atmosphere from analysis of Venus monitoring camera images, *Icarus*, *217*, 648–660, doi:10.1016/j.icarus.2011.08.008.

Peralta, J., R. Hueso, and A. Sánchez-Lavega (2007a), Cloud brightness distribution and turbulence in Venus using Galileo violet images, *Icarus*, *188*, 305–314, doi:10.1016/j.icarus.2006.12.005.

Peralta, J., R. Hueso, and A. Sánchez-Lavega (2007b), A reanalysis of Venus winds at two cloud levels from Galileo SSI images, *Icarus*, *190*, 469–477, doi:10.1016/j.icarus.2007.03.028.

Peralta, J., T. Imamura, P. L. Read, D. Luz, A. Piccialli, and M. A. López-Valverde (2014a), Analytical solution for waves in planets with atmospheric superrotation. I. Acoustic and inertia-gravity waves, *Astrophys. J.*, *213*(1), 17, doi:10.1088/0067-0049/213/1/17.

Peralta, J., T. Imamura, P. L. Read, D. Luz, A. Piccialli, and M. A. López-Valverde (2014b), Analytical solution for waves in planets with atmospheric superrotation. II. Lamb, surface, and centrifugal waves, *Astrophys. J.*, *213*(1), 18, doi:10.1088/0067-0049/213/1/18.

Rossow, W. B., A. D. del Genio, S. S. Limaye, and L. D. Travis (1980), Cloud morphology and motions from Pioneer Venus images, *J. Geophys. Res.*, *85*, 8107–8128.

Rossow, W. B., A. D. del Genio, and T. Eichler (1990), Cloud-tracked winds from Pioneer Venus OCPP images, *J. Atmos. Sci.*, *47*, 2053–2084.

Sánchez-Lavega, A. (2011), *An Introduction to Planetary Atmospheres*, Taylor and Francis, Boca Raton, Fla.

Schubert, G. (1983), *General Circulation and the Dynamical State of the Venus Atmosphere*, pp. 681–765, Univ. of Ariz. Press, Tucson.

Seiff, A., J. T. Schofield, A. J. Kliore, F. W. Taylor, and S. S. Limaye (1985), Models of the structure of the atmosphere of Venus from the surface to 100 kilometers altitude, *Adv. Space Res.*, *5*, 3–58, doi:10.1016/0273-1177(85)90197-8.

Smith, M. D., P. J. Gierasch, and P. J. Schinder (1992), A global traveling wave on Venus, *Science*, *256*, 652–655, doi:10.1126/science.256.5057.652.

Smith, M. D., P. J. Gierasch, and P. J. Schinder (1993), Global-scale waves in the Venus atmosphere, *J. Atmos. Sci.*, *50*, 4080–4096, doi:10.1175/1520-0469(1993)050<4080:GSWITV>2.0.CO;2.

Titov, D. V., F. W. Taylor, H. Svedhem, N. I. Ignatiev, W. J. Markiewicz, G. Piccioni, and P. Drossart (2008), Atmospheric structure and dynamics as the cause of ultraviolet markings in the clouds of Venus, *Nature*, *456*, 620–623, doi:10.1038/nature07466.

Titov, D. V., et al. (2012), Morphology of the cloud tops as observed by the Venus express monitoring camera, *Icarus*, *217*, 682–701, doi:10.1016/j.icarus.2011.06.020.

Yamamoto, M., and H. Tanaka (1997), Formation and maintenance of the 4-day circulation in the Venus middle atmosphere, *J. Atmos. Sci.*, *54*, 1472–1489, doi:10.1175/1520-0469(1997)054<1472:FAMOTD>2.0.CO;2.

Yamamoto, M., and H. Tanaka (1998), The Venusian Y-shaped cloud pattern based on an aerosol-transport model, *J. Atmos. Sci.*, *55*, 1400–1416, doi:10.1175/1520-0469(1998)055<1400:TVYSCP>2.0.CO;2.

Supporting Information for "Venus's major cloud feature as an equatorially trapped wave distorted by the wind"

DOI: 10.1002/2014GL062280

J. Peralta,[1] A. Sánchez-Lavega,[2,3] M. A. López-Valverde,[1,3] D. Luz[4], and P. Machado[4]

Contents of this file

1. Text S1

Additional Supporting Information (Files uploaded separately)

1. Caption for Figure S1
2. Caption for Movie S1

Introduction This Supporting Information includes the mathematical deduction of the equatorial wave solution presented in the main article (Text S1), a figure displaying the zonal wind profile used in our simulation (Figure S1) and the caption of video file with the animation for the wave distortion shown in Figure 3 (Movie S1).

[1]Instituto de Astrofísica de Andalucía (IAA-CSIC), Granada, Spain.

[2]Dep.Física Aplicada I, ETSI (UPV/EHU), Bilbao, Spain.

[3]Unidad Asociada GCP UPV/EHU-IAA(CSIC), Spain.

[4]Centro de Astronomia e Astrofísica da Universidade de Lisboa (CAAUL), Observatório Astronómico de Lisboa, Tapada da Ajuda, Lisboa, Portugal.

0094-8276/15/$5.00

Text S1.

1. Deducing the equatorially-trapped wave on Venus.

Considering Venus's large sidereal period jointly with its superrotating winds, a scale analysis reveals that the Coriolis terms are small compared with the metric terms corresponding to the centrifugal acceleration [*Schubert*, 1983], and for lower latitudes we obtain a system of equations that is closer to cyclostrophic equilibrium than to geostrophic. Additionally, we can also assume that the frictional force is negligible for all large-scale motions [*Peralta et al.*, 2014], that atmospheric motions are adiabatic in the upper cloud region [*Peralta et al.*, 2014], and that the atmosphere can be regarded as incompressible [*Covey and Schubert*, 1981; *Seiff*, 1982; *Izakov*, 2003]. The momentum, continuity and thermodynamic equations for the equatorial atmosphere of Venus will be:

$$\frac{Du}{Dt}+\frac{1}{\rho}\frac{\partial P}{\partial x} = \frac{u\cdot v}{a}\tan\phi \quad (1)$$

$$\frac{Dv}{Dt}+\frac{1}{\rho}\frac{\partial P}{\partial y} = -\frac{u^2}{a}\tan\phi \quad (2)$$

$$\frac{Dw}{Dt}+\frac{1}{\rho}\frac{\partial P}{\partial z} = -g \quad (3)$$

$$\frac{\partial u}{\partial x}+\frac{\partial v}{\partial y}+\frac{\partial w}{\partial z} = 0 \quad (4)$$

$$\frac{D\Theta}{Dt} = 0 \quad (5)$$

If we further apply the method of perturbations considering that the atmospheric density and pressure in their basic states have the forms [*Peralta et al.*, 2014] $\rho_0(z)$ and $P_0(y,z)$, and that the Venus atmosphere is at rest except for a background zonal wind $u_0(z)$ that varies only with altitude [*Peralta et al.*, 2014]:

$$\left(\frac{\partial u'}{\partial t}+u_0\frac{\partial u'}{\partial x}\right)+\frac{du_0}{dz}\cdot w'+\frac{\partial}{\partial x}\left(\frac{P'}{\rho_0}\right) = \Psi\cdot v' \quad (6)$$

$$\left(\frac{\partial v'}{\partial t}+u_0\frac{\partial v'}{\partial x}\right)+\frac{\partial}{\partial y}\left(\frac{P'}{\rho_0}\right) = -2\Psi\cdot u' \quad (7)$$

$$\left(\frac{\partial w'}{\partial t}+u_0\frac{\partial w'}{\partial x}\right)+\frac{\partial}{\partial z}\left(\frac{P'}{\rho_0}\right) = g\cdot\Theta' \quad (8)$$

$$\frac{\partial u'}{\partial x}+\frac{\partial v'}{\partial y}+\frac{\partial w'}{\partial z} = 0 \quad (9)$$

$$\left(\frac{\partial\Theta'}{\partial t}+u_0\frac{\partial\Theta'}{\partial x}\right)+\frac{N^2}{g}\cdot w' = 0 \quad (10)$$

where all the perturbations are a function of (x,y,z,t). The unknowns $[u',v',w']$ are the disturbed wind field components, $P'(x,y,z,t)$, $\rho(x,y,z,t)$ and $\Theta(x,y,z,t)$ are the perturbations for pressure, density and natural logarithm of the potential temperature ($\Theta\equiv\ln\theta$), N is the Brunt-Väisällä frequency ($N^2=g\cdot\partial\ln\theta/\partial z$), and we have introduced the new factor $\Psi\equiv(u_0/a)\cdot\tan\phi$ that will play in Venus a role similar to the Coriolis factor f on the Earth. *Peralta et al.* [2014] called this factor *centrifugal frequency*, with a being the Venus radius and ϕ the latitude.

To solve the wave equations at the equatorial region of Venus, we will simplify the system of equations (6-10) with assumptions equivalent to those employed by *Matsuno* [1966] for the terrestrial equatorial waves, although in this case we do not use the shallow water approach [*Sánchez-Lavega*, 2011]. These assumptions are: (a) the waves propagate exclusively in the west-east direction, with wave disturbances having the form $u'(x,y,z,t)=\hat{u}(y,z)\cdot\exp[i\cdot(k_{\rm x}x-\omega\,t)]$; (b) at the equator, $\phi=0$ and thus the centrifugal frequency is null $\Psi_0\cong 0$; (c) the β-plane approximation for the centrifugal frequency is valid on Venus equatorward of 45° (Fig. 1A in main article), and thus outside the equator the centrifugal frequency can be approximated by $\Psi\approx\beta_*\cdot y$ with $\beta_*=d\Psi/dy<0$ and about -10^{-12} s^{-1} m^{-1}.

Finally, assuming that ω is real (neutral waves), we can introduce in the wave expressions an intrinsic frequency ($\bar{\omega}=\omega-k_{\rm x}\cdot u_0$), thus obtaining the next set of equations in terms of the wave amplitudes for the equatorial region of Venus:

$$-i\bar{\omega}\cdot\hat{u}-\beta_*\cdot y\cdot\hat{v}+ik_{\rm x}\left(\frac{P'}{\rho_0}\right)+\frac{du_0}{dz}\cdot\hat{w} = 0 \quad (11)$$

$$-i\bar{\omega}\cdot\hat{v}+2\beta_*\cdot y\cdot\hat{u}+\frac{\partial}{\partial y}\left(\frac{\hat{P}}{\rho_0}\right) = 0 \quad (12)$$

$$\left(\bar{\omega}^2-N^2\right)\cdot\hat{w}+i\cdot\bar{\omega}\frac{\partial}{\partial z}\left(\frac{\hat{P}}{\rho_0}\right) = 0 \quad (13)$$

$$ik_{\rm x}\cdot\hat{u}+ik_{\rm y}\cdot\hat{v}+\frac{\partial\hat{w}}{\partial z} = 0 \quad (14)$$

where the wave amplitude for the potential temperature ($\hat{\Theta}$) in the vertical momentum (8) has been replaced by its expression in terms of $\hat{w}$ given in the thermodynamic equation (10). Thus, we have reduced our problem to a set of four equations with the four unknowns $\hat{u}(y,z)$, $\hat{v}(y,z)$, $\hat{w}(y,z)$ and $\hat{P}(y,z)$. The perturbed momentum equations (11) and (12) for a cyclostrophic regime are similar to the ones corresponding to a geostrophic one [see *Sánchez-Lavega*, 2011, eqs. 8.40a and 8.40b], except for the vertical shear of the zonal wind in equation (11), and the term $2\beta_*$ in 12) instead of the single $\beta=df/dy$ that is found in the geostrophic regime and where f is the Coriolis factor [*Sánchez-Lavega*, 2011].

1.1. Polarization relations for waves with $\bar{v}=0$.

In search for a Kelvin-like wave on Venus, we expect the centrifugal effect to play the same role as the Coriolis factor on the Earth, trapping and forcing a wave to move along the equator. For this reason, the wave amplitude for the meridional velocity must be zero everywhere ($\bar{v}=0$) hereafter. Moreover, estimations of the intrinsic phase velocity for the Venusian Kelvin wave have been found to range between $15-25$ m s^{-1} [*del Genio and Rossow*, 1990; *Kouyama et al.*, 2012], what implies that for a wave with planetary wavenumber 1 we can also assume that $\bar{\omega}^2\ll N^2$.

As a first step let us obtain a single differential equation in terms of only the wave amplitude $\hat{P}(y,z)$. Applying $\bar{v}=0$ and $\bar{\omega}^2\ll N^2$, we can solve $\hat{u}$ and $\hat{w}$ from (12) and (13) respectively, and replace them in (11) to obtain:

$$\frac{1}{y}\cdot\frac{\partial}{\partial y}\left(\frac{\hat{P}}{\rho_0}\right)+\left(\frac{2\beta_*}{\bar{\omega}/k}\right)\cdot\frac{\hat{P}}{\rho_0}+\left(\frac{2\beta_*}{N^2}\frac{du_0}{dz}\right)\cdot\frac{\partial}{\partial z}\left(\frac{\hat{P}}{\rho_0}\right)=0 \quad (15)$$

Provided that $du_0/dz = 0$ also occurs in the atmospheric region of interest (Fig. 1B in main article) then, considering that $\beta_* < 0$ and introducing the intrinsic phase velocity $\bar{c}_x = \bar{\omega}/k$, the solution of (15) when $du_0/dz = 0$ is:

$$\bar{P} \propto \exp\left[\left(\frac{|\beta_*|}{\bar{c}_x}\right)\cdot y^2\right] \tag{16}$$

For the general case $du_0/dz \neq 0$, we assume for simplicity that du_0/dz, β_* and N^2 are not a function of the meridional coordinate y. The cases of du_0/dz and β_* are justified by Figs. 1B and 1A in main article, while for N^2 we assume that it is constant but with error bars accounting for its small variation with latitude. Also considering that β_* does not vary strongly with altitude(Fig. 1A), we can assume that $\hat{P}/\rho_0 = \hat{P}_y(y)\cdot\Phi(z)$ with $\Phi(z) = \hat{P}_z(z)\cdot e^{imz}$. Conveniently manipulating (15), we can obtain an equation where one side depends only on y and the other on z. In this case, both sides must be equal to a constant (Γ^2) to be chosen for convenience, thus obtaining the separated equations:

$$\frac{1}{y}\cdot\frac{\partial \ln \hat{P}_y}{\partial y} + \left(\frac{2\beta_*}{\bar{\omega}/k}\right) = -\Gamma^2 \tag{17}$$

$$\left(\frac{2\beta_*}{N^2}\right)\cdot\frac{du_0}{dz}\cdot\frac{\partial \ln \Phi(z)}{\partial z} = \Gamma^2 \tag{18}$$

and thus the solutions are:

$$\hat{P}_y = \exp\left[-\left(\frac{\Gamma^2}{2} + \frac{|\beta_*|}{|\bar{c}_x|}\right)\cdot y^2\right] \tag{19}$$

$$\hat{P}_z = \exp\left[-\frac{\Gamma^2}{2|\beta_*|}\cdot\int_{z_0}^{z} dz\frac{N^2}{du_0/dz}\right] \tag{20}$$

where z_0 is the reference altitude where $du_0/dz = 0$ (see Fig. 1B in main article) and we already considered that $\bar{c}_x < 0$. Note that the solutions (19) and (20) provide the horizontal and vertical modulation for the wave amplitude. The constant Γ^2 is, in fact, linked to the existence of vertical shear for the background zonal wind and disappears when $du_0/dz = 0$. Also observe that above and below the altitude $z = z_0$ we have $du_0/dz > 0$ and $du_0/dz < 0$ respectively, so it is direct to deduce that the wave amplitude decays exponentially up and down from the region where the zonal wind peaks. From this, we can easily derive expressions for the horizontal and vertical e-folding decays of the wave amplitude:

$$\theta^H_{\mathrm{e-fold}} = \left(\frac{\Gamma^2}{2} + \frac{|\beta_*|}{|\bar{c}_x|}\right)^{-1/2} \tag{21}$$

$$\theta^V_{\mathrm{e-fold}} = \frac{2|\beta_*|}{\Gamma^2}\cdot\frac{|du_0/dz|}{N^2} \tag{22}$$

Finally, considering (12) and (13) we can finally obtain the polarization relations:

$$\begin{aligned}\hat{P} =& \hat{P}_0\cdot\exp\left[-\left(\frac{\Gamma^2}{2} + \frac{|\beta_*|}{|\bar{c}_x|}\right)\cdot y^2\right] \\ &\cdot\exp\left[\frac{-\Gamma^2}{2|\beta_*|}\int_{z_0}^{z} dz\frac{N^2}{du_0/dz}\right]\cdot e^{imz}\end{aligned} \tag{23}$$

$$\hat{u} = \left(\frac{\Gamma^2}{2|\beta_*|} + \frac{1}{|\bar{c}_x|}\right)\cdot e^{i\cdot\pi}\cdot\frac{\hat{P}}{\rho_0} \tag{24}$$

$$\hat{w} = \left(\frac{|\bar{\omega}|}{N^2}m\right)\cdot\frac{\hat{P}}{\rho_0} + \left(\frac{\Gamma^2}{2|\beta_*|}\cdot\frac{|\bar{\omega}|}{du_0/dz}\right)\cdot e^{i\frac{\pi}{2}}\cdot\frac{\hat{P}}{\rho_0} \tag{25}$$

where $\hat{P}_0 = \hat{P}(0, z_0)$. As it can be seen from (23-24), both zonal and vertical velocity wave disturbances are phase-shifted relative to the pressure disturbances. P' and u' are phase shifted π radians, while w' has a component in phase with P' and another one shifted $\pi/2$ relative to P' (eqs. 23 and 25).

1.2. Dispersion relation for waves with $\bar{v} = 0$.

Going back to equations (11-14) and applying again that $\bar{v} = 0$ and $\bar{\omega}^2 \ll N^2$, it is possible to derive an equation that will allow us to derive for the dispersion relation for these new waves on Venus. Calculating $k\cdot(11)+\bar{\omega}\cdot(14)$ we obtain:

$$\bar{\omega}\frac{\partial\hat{w}}{\partial z} + k\frac{du_0}{dz}\cdot\hat{w} + ik^2\left(\frac{\hat{p}}{\rho_0}\right) = 0 \tag{26}$$

And equation (26) can be combined with the vertical momentum equation (13) by calculating the quantity $+\bar{\omega}\partial/\partial z\cdot(26) + k^2\cdot(13)$, thus obtaining the following second-order differential equation:

$$\frac{\partial^2\hat{w}}{\partial z^2} + \left[\frac{k}{\bar{\omega}}\left(\frac{du_0}{dz}\right)\right]\cdot\frac{\partial\hat{w}}{\partial z} + \left[\frac{k}{\bar{\omega}}\left(\frac{d^2u_0}{dz^2}\right) + \frac{k^2}{\bar{\omega}^2}N^2\right]\cdot\hat{w} = 0 \tag{27}$$

This second-order differential equation can be reduced to another one with no first derivatives by using the change of variables $\hat{w}(y,z) = \tilde{w}(y,z)\cdot\exp\left[-\frac{1}{2}\left(\frac{k}{\bar{\omega}}\frac{du_0}{dz}\right)\cdot z\right]$. In those height interval for which $du_0/dz \neq 0$ and $d^2u_0/dz^2 = 0$, the dispersion relation is found to be:

$$\bar{\omega} = \frac{-k}{\sqrt{k^2+m^2}}\cdot\sqrt{N^2 - \frac{1}{4}\left(\frac{du_0}{dz}\right)^2} \tag{28}$$

$$\bar{c_x} = \frac{-1}{\sqrt{k^2+m^2}}\cdot\sqrt{N^2 - \frac{1}{4}\left(\frac{du_0}{dz}\right)^2} \tag{29}$$

that can be written in terms of the Richardson number $Ri = N^2/(du_0/dz)$:

$$\bar{\omega} = \frac{-k}{\sqrt{k^2+m^2}}\cdot\left|\frac{du_0}{dz}\right|\cdot\sqrt{Ri - 1/4} \tag{30}$$

And the intrinsic frequency will be real only if the Richardson number $Ri > 1/4$, which is the condition for not having dynamical or convective instability [*Gubenko et al.*, 2008].

Figure S1. Zonal wind profile used to simulate how the Kelvin-like wave is distorted by the wind in comparison with the time evolution of the Y-feature during the Pioneer Venus mission (see Figure 3 in main article). The model background wind is displayed with a continuous black line, while the zonal wind measurements during the Pioneer Venus observations are displayed with blue circles [*Rossow et al.*, 1980].

Movie S1. Animation displaying the equatorial wave deformation due to Venus's zonal winds. The propagation of the equatorial wave predicted by our analytical model is simulated within a realistic profile of the zonal winds of Venus during Pioneer Venus observations (fs01.eps). The simulation has been carried out projecting the wave structure over a sphere, using time steps of 0.1 terrestrial days and along a time span of 30 days. An intrinsic phase velocity of about 14 m s^{-1} was used to fit Pioneer Venus estimations, while for the background zonal wind constant between the equator and midlatitudes we chose a mean value from Pioneer Venus observations. The wave phase expected to exhibit the high concentrations of the absorber due to the upwelling are displayed with a single tone of black, while the phase associated to the downwelling and where wave's amplitude is less than 1% of the maximum, are displayed in white to enhance contrast.

References

Covey, C. C., and G. Schubert (1981), 4-day waves in the Venus atmosphere, *Icarus*, *47*, 130–138, doi:10.1016/0019-1035(81)90097-X.

del Genio, A. D., and W. B. Rossow (1990), Planetary-scale waves and the cyclic nature of cloud top dynamics on Venus, *Journal of Atmospheric Sciences*, *47*, 293–318.

Gubenko, V. N., A. G. Pavelyev, and V. E. Andreev (2008), Determination of the intrinsic frequency and other wave parameters from a single vertical temperature or density profile measurement, *Journal of Geophysical Research (Atmospheres)*, *113*, D08109, doi:10.1029/2007JD008920.

Izakov, M. N. (2003), Estimating the Role of Different Sources of Turbulent Energy in the Atmosphere of Venus, *Solar System Research*, *37*, 489–496, doi:10.1023/B:SOLS.0000007947.51720.ed.

Kouyama, T., T. Imamura, M. Nakamura, T. Satoh, and Y. Futaana (2012), Horizontal structure of planetary-scale waves at the cloud top of Venus deduced from Galileo SSI images with an improved cloud-tracking technique, *Planetary and Space Science*, *60*, 207–216, doi:10.1016/j.pss.2011.08.008.

Matsuno, T. (1966), Quasi-geostrophic motions in the equatorial area, *Journal of the Meteorological Society of Japan*, *44*, 25–43.

Peralta, J., T. Imamura, P. L. Read, D. Luz, A. Piccialli, and M. A. López-Valverde (2014a), Analytical solution for waves in planets with atmospheric superrotation. i. acoustic and inertia-gravity waves, *The Astrophysical Journal Supplement Series*, *213*(1), 17, doi:10.1088/0067-0049/213/1/17.

Rossow, W. B., A. D. del Genio, S. S. Limaye, and L. D. Travis (1980), Cloud morphology and motions from Pioneer Venus images, *Journal of Geophysical Research*, *85*, 8107–8128.

Sánchez-Lavega, A. (2011), *An Introduction to Planetary Atmospheres*, Taylor & Francis.

Schubert, G. (1983), *General circulation and the dynamical state of the Venus atmosphere*, pp. 681–765.

Seiff, A. (1982), Dynamical implications of the observed thermal contrasts in Venus' upper atmosphere, *Icarus*, *51*, 574–592, doi:10.1016/0019-1035(82)90147-6.

Corresponding author: J. Peralta, Instituto de Astrofísica de Andalucía, Glorieta de la Astronomía s/n, Granada, 18008, SPAIN. (peralta@iaa.es)

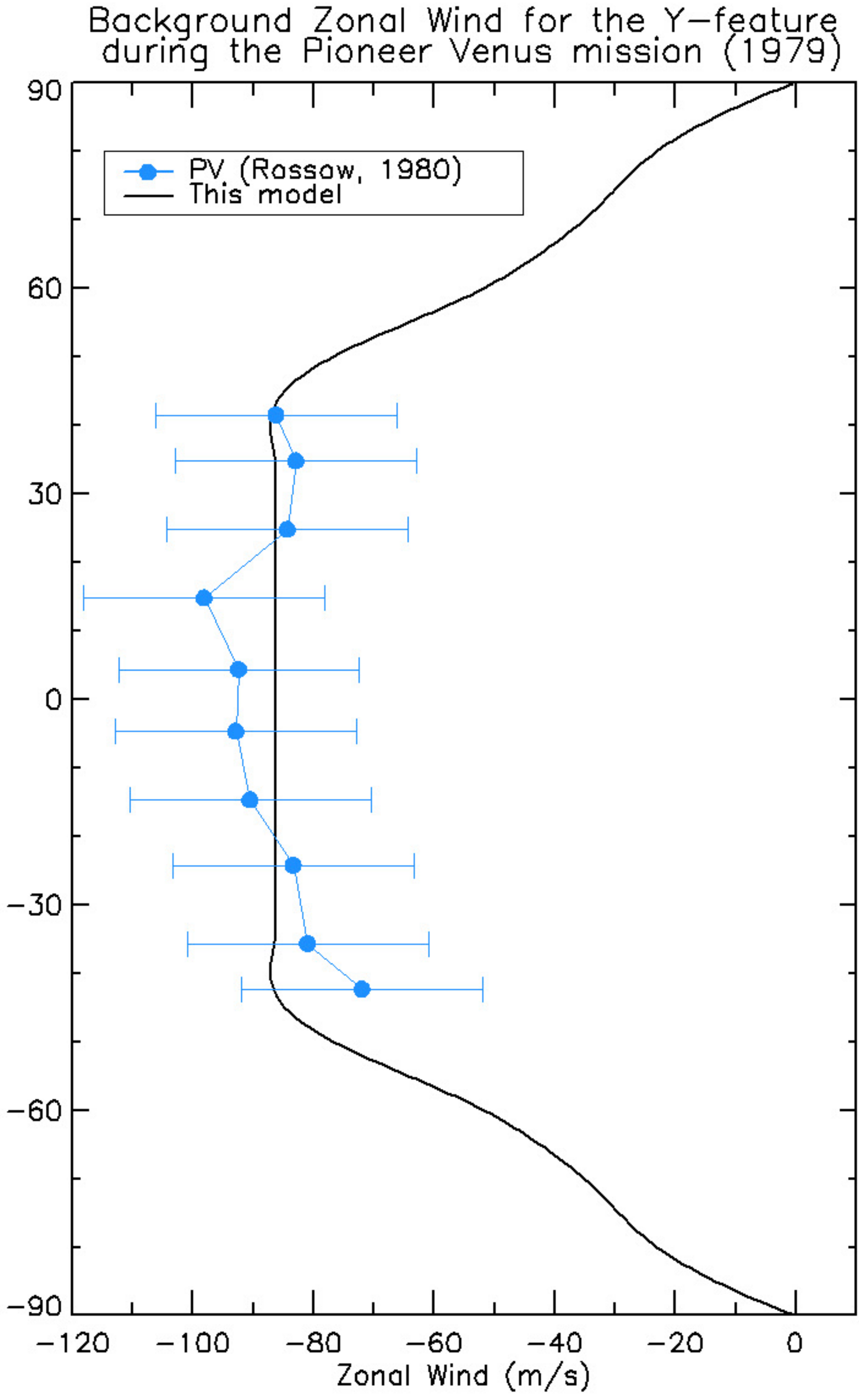
Background Zonal Wind for the Y-feature
during the Pioneer Venus mission (1979)
PV (Rossow, 1980)
This model
90
60
30
0
−30
−60
−90
Latitude
−120
−100
−80
−60
−40
−20
0
Zonal Wind (m/s)